Published in final edited form as:

J Biol Chem. 2004 February 27; 279(9): 7999–8010. doi:10.1074/jbc.M308281200.

The Role of Phosphorylation in D_1 Dopamine Receptor Desensitization:

EVIDENCE FOR A NOVEL MECHANISM OF ARRESTIN ASSOCIATION

Ok-Jin Kim[‡,§], **Benjamin R. Gardner**[‡,§,¶], **Daniel B. Williams**[‡,‖], **Paul S. Marinec**[‡], **David M. Cabrera**[‡], **Jennifer D. Peters**[‡,**], **Chun C. Mak**[‡], **Kyeong-Man Kim**[‡‡], and **David R. Sibley**[‡,§§]

[‡]Molecular Neuropharmacology Section, NINDS, National Institutes of Health, Bethesda, Maryland 20892-1406

[‡‡]College of Pharmacy, Chonnam National University, KwangJu, 500-757, Korea

Abstract

Homologous desensitization of D_1 dopamine receptors is thought to occur through their phosphorylation leading to arrestin association which interdicts G protein coupling. In order to identify the relevant domains of receptor phosphorylation, and to determine how this leads to arrestin association, we created a series of mutated D_1 receptor constructs. In one mutant, all of the serine/threonine residues within the 3rd cytoplasmic domain were altered (3rdTOT). A second construct was created in which only three of these serines (serines 256, 258, and 259) were mutated (3rd234). We also created four truncation mutants of the carboxyl terminus (T347, T369, T394, and T404). All of these constructs were comparable with the wild-type receptor with respect to expression and adenylyl cyclase activation. In contrast, both of the 3rd loop mutants exhibited attenuated agonist-induced receptor phosphorylation that was correlated with an impaired desensitization response. Sequential truncation of the carboxyl terminus of the receptor resulted in a sequential loss of agonist-induced phosphorylation. No phosphorylation was observed with the most severely truncated T347 mutant. Surprisingly, all of the truncated receptors exhibited normal desensitization. The ability of the receptor constructs to promote arrestin association was evaluated using arrestin-green fluorescent protein translocation assays and confocal fluorescence microscopy. The 3rd234 mutant receptor was impaired in its ability to induce arrrestin translocation, whereas the T347 mutant was comparable with wild type. Our data suggest a model in which arrestin directly associates with the activated 3rd cytoplasmic domain in an agonist-dependent fashion; however, under basal conditions, this is sterically prevented by the carboxyl terminus of the receptor. Receptor activation promotes the sequential phosphorylation of residues, first within the carboxyl terminus and then the 3rd cytoplasmic loop, thereby dissociating these domains and allowing arrestin to bind to the activated 3rd loop. Thus, the role of receptor

[§§]To whom correspondence should be addressed: Molecular Neuropharmacology Section, NINDS/National Institutes of Health, Bldg. 10, Rm. 5C108, 10 Center Dr., MSC 1406, Bethesda, MD 20892-1406. Tel.: 301-496-9316; Fax: 301-496-6609; sibley@helix.nih.gov.

[§]Both authors contributed equally to this work.

[¶]Present address: Pfizer Ltd., Ramsgate Rd., Sandwich, Kent CT13 9NJ, UK.

[‖]Present address: Dept. of Natural Sciences, New Mexico Highlands University, Las Vegas, NM 87701.

[**]Present address: Dept. of Psychology, Princeton University, Princeton, NJ 08544.

The on-line version of this article (available at http://www.jbc.org) contains movies.

phosphorylation is to allow *access* of arrestin to its receptor binding domain rather than to create an arrestin binding site *per se*.

Agonist activation of most G protein-coupled receptors (GPCRs)[1] is quickly followed by homeostatic processes that desensitize or return the receptor activity back toward basal levels (reviewed in Refs. 1–3). Desensitization of GPCRs is thought to largely involve their phosphorylation by a variety of protein kinases. One category of protein kinases, involved in heterologous desensitization, are those activated by second messengers, such as cAMP-dependent protein kinase or protein kinase C. Phosphorylation of GPCRs by these kinases does not require agonist occupancy and results in reduced G protein coupling. A second category of protein kinases are the GPCR kinases (GRKs) that mediate homologous desensitization of GPCRs. Phosphorylation of GPCRs by GRKs is strictly dependent on agonist occupancy resulting in desensitization of only those receptors that were activated. GRK phosphorylation generally occurs on serine and/or threonine residues in the GPCR carboxyl terminus and/or 3rd cytoplasmic loop. Phosphorylation by GRKs has been shown to decrease the affinity of the GPCR for its cognate G protein and also results in the binding of an arrestin protein. Arrestin association further prohibits G protein coupling and also targets the GPCR for endocytosis. Once internalized, the GPCR can engage additional signaling pathways and be sorted for recycling to the plasma membrane or targeted for degradation (1–3). Although this basic desensitization paradigm may be operative for most G protein-coupled receptors, it is becoming apparent that there may be significant exceptions and widespread variations on this general scheme.

One area of significant complexity is the mechanism by which GRK phosphorylation leads to arrestin association with the GPCR. Surprising little is known about this process with most information coming from the rhodopsin-visual arrestin system. Gurevich and co-workers (4, 5) have proposed a model whereby arrestin binds to the phosphorylated carboxyl terminus of rhodopsin resulting in the disruption of intramolecular forces within the arrestin protein leading to an altered conformation with high affinity for rhodopsin. By using constitutively active mutants of arrestins, Gurevich and co-workers (6, 7) have also provided evidence that this model may be applicable to the β_2-adrenergic receptor that also undergoes GRK-mediated phosphorylation on its carboxyl terminus. Despite these advances, it is not clear if this model is generally applicable to all GPCR/arrestin interactions, particularly for GPCRs that do not undergo GRK phosphorylation on their carboxyl termini. Remaining unclear for the vast majority of GPCRs is the precise number, location, and role of GRK phosphorylation sites that lead to arrestin association and ultimately desensitization.

Like most GPCRs, the D_1 dopamine receptor undergoes both second messenger and GRK-mediated phosphorylation reactions that lead to its desensitization. Conflicting evidence has been provided as to the relative role of second messenger activated protein kinases, primarily PKA, and that of GRK-mediated phosphorylation (reviewed in Ref. 8). In some systems, agonist-induced phosphorylation of the D_1 receptor appears to be mediated

[1]The abbreviations used are: GPCRs, G protein-coupled receptors; GRK, G protein-coupled receptor kinase; PKA, protein kinase A; DMEM, Dulbecco's modified essential medium; FCS, fetal calf serum; EBSS, Earle's balanced salt solution; WT, wild type; GFP, green fluorescent protein; CHO, Chinese hamster ovary.

predominantly by PKA (9), whereas in others GRKs appear to play a primary role (10–13). Similarly, the exact sites of phosphorylation are unclear. Both Jiang and Sibley (14) and Mason *et al.* (9) have provided evidence that T268 in the 3rd cytoplasmic loop of the D_1 receptor is phosphorylated in a PKA-dependent fashion and that this regulates either the rate of desensitization (14) or intracellular trafficking of the receptor once internalized (9). In contrast, Jackson *et al.* (15) have provided evidence that the D_1 receptor is primarily phosphorylated on multiple residues within its carboxyl terminus. Similarly, Lamey *et al.* (13) have provided evidence that agonist-induced phosphorylation of the human D_1 receptor is restricted to the carboxyl terminus; however, they report that only a single residue, T360, is involved and that this is likely phosphorylated by a GRK. This finding conflicts with a previous observation by Tiberi *et al.* (10) that GRK-mediated phosphorylation of the D_1 receptor takes place exclusively on serine residues. Many of these studies utilized different cellular host systems for receptor expression, suggesting that this might account for some of these disparate results.

Because Tiberi *et al.* (10) have shown that phosphorylation of the D_1 receptor in HEK293 cells is predominantly mediated by GRK(s) and because we are interested in mapping the functionally relevant domains of GRK-mediated phosphorylation and determining how this leads to arrestin association, we have used these cells in our current study. We now provide evidence for functionally relevant phosphorylation sites within both the 3rd cytoplasmic loop and the carboxyl terminus of the D_1 receptor and that phosphorylation of both of these domains is required for rapid association of arrestin with the receptor. Rather than the creation of an arrestin binding site *per se*, however, the only role of receptor phosphorylation is to alter the conformation of the 3rd cytoplasmic loop and/or the carboxyl terminus such that arrestin can associate with and bind to the activated 3rd cytoplasmic domain.

EXPERIMENTAL PROCEDURES

Materials

HEK293 cells were purchased from American Type Culture Collection (Manassas, VA). HEK293-tsa201 (HEK293T) cells (16) were a gift of Dr. Vanitha Ramakrishnan. [^{3}H]SCH-23390 (70–71.3 Ci/mmol) and [^{3}H]cAMP (31.4 Ci/mmol) were obtained from Diagnostic Products Corp. (Los Angeles, CA). [^{32}P]Orthophosphate (carrier-free) was obtained from Amersham Biosciences. Dopamine, Ro-20-1724, (±)-propranolol, and (+)-butaclamol were purchased from Research Biochemicals Inc. (Natick, MA). Cyclic AMP assay kits were from Diagnostic Products Corp. (Los Angeles, CA). Cell culture media and reagents were from Invitrogen. Fetal calf serum was purchased from Summit Biotechnology (Purchase, CO). Calcium phosphate transfection kits were from Invitrogen. MiniComplete™ protease inhibitor mixture was purchased from Roche Applied Science. M2-affinity gel and all other reagents were purchased from Sigma.

Cell Culture and Transfections

HEK293 and HEK293T cells were cultured in Dulbecco's modified essential medium (DMEM) supplemented with 10% fetal calf serum, 1 mM sodium pyruvate, 50 units/ml

penicillin, 50 μg/ml streptomycin, and 10 μg/ml gentamycin. Cells were grown at 37 °C in 5% CO_2 and 90% humidity. An amino-terminal FLAG epitope-tagged construct of the rat D_1 receptor (17) was created from pSFβ_2, an expression construct containing a FLAG-tagged β_2-adrenergic receptor (18). The β_2-adrenergic receptor sequence was excised using NcoI and SalI, and following NcoI/SalI digestion of the rat D_1 receptor sequence, the D_1 receptor was inserted in-frame 3′ to the FLAG epitope sequence to create pSFD_1, as reported previously (12). This construct, and mutants thereof, were used for all experiments except for the confocal fluorescence microscopy experiments shown in Figs. 12 and 13. Similarly, HEK293-tsa201 (HEK293T) cells were used for all experiments except for those shown in Figs. 12 and 13, which employed regular HEK293 cells. Site-directed mutagenesis was performed using a QuickChange kit from Stratagene (La Jolla, CA). Truncated receptors were created by generating stop codons at the indicated locations (Fig. 1) in the protein sequence. All constructs were verified by DNA sequencing prior to use. HEK293 or HEK293T cells were transfected using the calcium phosphate precipitation method (Invitrogen). Cells were seeded in 100- or 150-mm^2 plates, and transfection was carried out at ~50% confluency. DNA and 60 μl of 2 M $CaCl_2$ were mixed in H_2O in a total volume of 1 ml and then slowly mixed with HEPES-buffered saline. The reaction mixture was incubated at room temperature for 25 min and then evenly added to the cell culture dish containing 20 ml of fresh media. After 18 h, the transfection media were replaced with fresh media, and the cells were divided for subsequent experiments.

Radioligand Binding Assays

HEK293T cells were harvested by incubation with 5 mM EDTA in Earle's balanced salt solution (EBSS) and collected by centrifugation at 300 × *g* for 10 min. The cells were resuspended in lysis buffer (5 mM Tris, pH 7.4, 4 °C; 5 mM $MgCl_2$) and were disrupted using a Dounce homogenizer followed by centrifugation at 34,000 × *g* for 10 min. The resulting membrane pellet was resuspended in binding buffer (50 mM Tris, pH 7.4). The membrane suspension (final protein concentration = 20 μg/tube) was then added to assay tubes containing [^{3}H]SCH-23390 in a final volume of 1.0 ml. (+)-Butaclamol was added at the final concentration of 3 μM to determine nonspecific binding. The assay tubes were incubated at room temperature for 1 h, and the reaction was terminated by rapid filtration through GF/C filters pretreated with 0.3% polyethyleneimine. Radioactivity bound to the filters was quantitated by liquid scintillation spectroscopy at a counting efficiency of 47%.

Determination of cAMP Production

HEK293T cells were seeded into 24-well plates (150,000 cells per well) and cultured for 1 day prior to the experiment. To assess desensitization, the cultures were first pretreated for the indicated times in the absence or presence of dopamine with 0.1 mM L-ascorbic acid and 5 μM (±)-propranolol (to block endogenous β-adrenergic receptors) and in HDMEM (20 mM HEPES-buffered DMEM, pH 7.4, 37 °C). Subsequently, the cells were washed four times with 400 μl of EBSS (37 °C) and were further incubated with various concentrations of dopamine in a total volume of 250 μl at 37 °C for 15 min in the presence of 30 μM Ro-20-1724, 100 μM L-ascorbic acid, and 5 μM (±)-propranolol. The reaction was terminated by discarding the supernatant and adding 200 μl of 3% perchloric acid per well. After incubating on ice for 30 min, 80 μl of 15% $KHCO_3$ was added to the wells, and the plates

were further incubated for 10 min. The plates were then centrifuged for 10 min at 1,300 × *g*, and 50 μl of the supernatant from each well was subsequently transferred to a 1.2-ml tube containing 250 μl of reaction mixture (150 μl of Tris-EDTA buffer, 50 μl of cAMP-binding protein, and 50 μl of [^{3}H]cAMP). After incubation at 4 °C overnight, 250 μl of charcoal/dextran mix (1%) was added to each tube followed by incubation at 4 °C for 15 min and then centrifugation for 15 min at 1,300 × *g*. Radioactivity in the supernatant from each tube was quantified by liquid scintillation spectroscopy at a counting efficiency of 47%. Cyclic AMP concentrations were calculated using a standard curve according to the protocol of the assay kit.

Whole Cell Phosphorylation Assays

These were performed as described previously (12). Briefly, 1 day prior to the experiment, HEK293T cells were seeded at 1 × 10^6 per well of a 6-well plate and cultured overnight. Cells were then washed with EBSS and incubated for 1 h in phosphate-free DMEM. Media were then removed and replaced with 2 ml of fresh media supplemented with 200 μCi/ml carrier-free [^{32}P]H_3PO_4. After 90 min at 37 °C, the cells were then challenged with dopamine in media supplemented with 100 μM L-ascorbic acid for the times and concentrations described in the text. Cells were then transferred to ice, washed twice with ice-cold EBSS, and solubilized for 1 h at 4 °C in 1 ml of solubilization buffer (50 mM HEPES, 1 mM EDTA, 10% glycerol, 1% Triton X-100, pH 7.4, 4 °C) + 150 mM NaCl supplemented with MiniComplete™ protease mixture, 0.1 mM phenylmethylsulfonyl fluoride, and phosphatase inhibitors (5 mM sodium pyrophosphate, 50 mM NaF). The samples were cleared by centrifugation in a microcentrifuge, and the protein concentration was determined by a BCA protein assay (Pierce). In each experiment, the level of receptor expression for each construct was quantified via radioligand binding assays using cells from duplicate wells that were treated identically except for the addition of [^{32}P]H_3PO_4. After receptor/protein quantification, equal amounts of solubilized receptor protein were then transferred to fresh tubes with 50 μl of washed M2-affinity gel and incubated overnight with mixing at 4 °C. The samples were then washed once with solubilization buffer + 500 mM NaCl, once with solubilization buffer + 150 mM NaCl, and once with TE (Tris-EDTA, pH 7.4, 4 °C). Samples were then incubated in 2× SDS-PAGE loading buffer for 1 h at 37 °C before being resolved by 8% SDS-PAGE. The gels were dried and subjected to autoradiography. All assays included cells challenged with vehicle as an internal control.

Cell Surface Biotinylation Assays

HEK293T cells were transfected with the indicated D_1 receptor constructs using the calcium phosphate precipitation method and were seeded in poly-D-lysine-coated plates 1 day prior to the whole cell biotinylation experiment. The level of receptor expression for each construct was determined by radioligand binding assays in cells from duplicate plates as described above. Cells were washed three times with cold phosphate-buffered saline and treated with 1 mg/ml biotin (Pierce) in phosphate-buffered saline for 15 min at 37 °C. After the whole cell biotinylation, the cells were washed three times with phosphate-buffered saline and harvested with 1 ml of solubilization buffer (50 mM HEPES, 1 mM EDTA, 10% glycerol, 1% Triton X-100, pH 7.4, 4 °C) supplemented 150 mM NaCl with protease inhibitor mixture (Roche Applied Science). After a 1-h incubation on ice, the samples were cleared by

centrifugation, and the protein concentration was determined by BCA protein assay (Pierce). Equal amounts of receptor protein, as determined for the phosphorylation assays, were then transferred to fresh tubes with 50 μl of washed M2-affinity gel and incubated overnight with rotation at 4 °C. The samples were then washed once with solubilization buffer + 500 mM NaCl, once with solubilization buffer + 150 mM NaCl, and once with TE (Tris-EDTA, pH 7.4, 4 °C). Samples were then incubated in 2× SDS-PAGE loading buffer for 1 h at 37 °C before being resolved on a 4–12% gradient SDS-PAGE mini-gel. The proteins from the gel were transferred to polyvinylidene difluoride membrane for 30 min at 25 V. The polyvinylidene difluoride membrane was washed with TBST (Tris-buffered saline + 0.1% Tween 20) three times and incubated with Vectastain ABC reagents (Vector Laboratories) for 1 h. The membrane was washed with TBST four times and developed using with SuperSignal West Pico chemiluminescent detection system (Pierce). The relative intensities of biotinylated bands were determined by scanning densitometry and analysis using the software program NIH Image.

Confocal Microscopy and Arrestin-GFP Translocation Assays

In order to obtain increased receptor expression in regular HEK293 cells, we excised the entire expression cassettes from the $pSFD_1$ vector (harboring either the wild-type or mutant D_1 receptors) using HindIII and SalI and subcloned them into expression vector pCMV5 (19; a gift from Dr. Marc G. Caron). For confocal microscopy, 3×10^5 HEK293 cells were seeded in 60-mm^2 culture plates, and 24 h later, each plate was transfected with 5 μg of receptor DNA and 1 μg of either arrestin2-GFP or arrestin3-GFP (gifts from Dr. Marc G. Caron). Twenty-four hours post-transfection, cells were plated on 35-mm glass bottom culture dishes. Two hours prior to stimulation, the medium was replaced with serum-free DMEM supplemented with 10 mM HEPES. Confocal microscopy was performed on a Zeiss laser-scanning confocal microscope (LSM-510). Images were collected sequentially every 30 s after agonist stimulation with 20 μM dopamine using single line excitation (488 nm).

Data Analysis

All binding assays were routinely performed in triplicate and were repeated three to four times. Cyclic AMP experiments were performed in duplicate and were repeated three to four times. Estimation of the radioligand binding parameters, K_D and B_{max}, as well as the EC_{50} values for dopamine stimulation of cAMP production were calculated using the GraphPad Prizm curve-fitting program. The curves presented throughout this paper, representing the best fits to the data, were generated using this software program as well. The relative intensities of phosphorylated bands were determined by scanning the autoradiographs and analyzing using the software program NIH Image.

RESULTS

Expression of Wild-type and Mutated D_1 Receptors in HEK293T Cells

In order to identify the functionally relevant sites of phosphorylation in the D_1 receptor and to determine how phosphorylation leads to arrestin association and desensitization, we created a series of mutated D_1 receptor constructs. Because multiple phosphorylation sites have been mapped to both the 3rd cytoplasmic domain and carboxyl termini of most

GPCRs, we decided to focus on these regions within the D_1 receptor protein. Fig. 1 shows a diagram of the rat D_1 receptor and all of the mutated receptors used in this study. We created two mutant constructs with altered residues within the 3rd cytoplasmic domain. One of these, termed the 3rd TOTAL (3rdTOT) mutant, had all of the serine and threonine residues within the 3rd cytoplasmic loop simultaneously changed to either alanine or valine, as indicated (Fig. 1). The other mutant receptor, termed 3rd234, had only three of the serine residues in the 3rd cytoplasmic loop (Ser-256, Ser-258, and Ser-259) simultaneously mutated to alanines. We also created four truncation mutants of the carboxyl terminus (T347, T369, T394, and T404). This was accomplished by engineering stop codons such that the receptor protein was truncated at the indicated locations (Fig. 1).

We initially evaluated the expression of the various receptor constructs by transiently expressing them in HEK293T cells. Fig. 2 shows a single experiment in which all of the constructs were simultaneously expressed and saturation binding isotherms constructed using [^{3}H]SCH-23390, a radiolabeled D_1 receptor antagonist. We found that all of the mutant receptors were expressed at a similar level as the wild-type receptor with the exception of the most severely truncated receptor, T347, which consistently expressed at about one-third the level of the WT construct. No difference in affinity for [^{3}H]SCH-23390 was noted for any of the receptor constructs.

We next evaluated the functional activity of the D_1 receptor constructs by examining their ability to activate adenylate cyclase and raise intracellular levels of cAMP. Fig. 3 shows an experiment in which all of the receptors were simultaneously expressed, and dose-response curves for dopamine stimulation of cAMP accumulation were constructed. All of the mutant receptors were able to stimulate intracellular cAMP accumulation to the same degree as the wild-type receptor. Similarly, all of the mutant receptors, with the exception of the 3rdTOT construct, exhibited an identical potency for dopamine. The 3rdTOT receptor consistently showed an approximate 3–4-fold rightward shift in the dopamine dose-response curve.

In order to establish that the transiently transfected D_1 receptor will exhibit significant agonist-induced desensitization in the HEK293T cells, we performed the experiment shown in Fig. 4. HEK293T cells expressing the wild-type D_1 receptor were pretreated with dopamine for the indicated times and washed, and then cAMP accumulation was examined in response to dopamine. Dopamine pretreatment indeed resulted in desensitization of the subsequent dopamine response as manifested by a reduction (of about 40%) in the maximum cAMP accumulation as well as an ~2-fold rightward shift in the dose-response curve. Maximum desensitization of the D_1 receptor response was observed to occur by about 1 h of dopamine pretreatment.

Phosphorylation and Desensitization of the 3rd Cytoplasmic Loop Mutants

To examine directly the phosphorylation status of the D_1 receptor constructs, the HEK293Tcells were metabolically labeled with [^{32}P]H_3PO_2 followed by solubilization and immunopurification of the receptor. Fig. 5*A* shows an autoradiogram of immunoprecipitates from metabolically labeled and transfected cells treated with or without dopamine. The phosphorylated protein with a molecular mass of about 55–60 kDa represents the D_1 receptor, as this protein was not observed in non-transfected cells (data not shown). As can

be seen, the D_1 receptor is phosphorylated under basal conditions, and its phosphorylation state is increased 2–3-fold upon agonist pretreatment. These results are similar to those previously observed by us using C6 glioma cells (12). Interestingly, both of the receptor constructs with serine and/or threonine mutations within the 3rd cytoplasmic loop appear to exhibit diminished phosphorylation in both the basal and dopamine-stimulated state. Fig. 5*B* shows summary data from several experiments in which the phosphorylation data were quantified. Both of the 3rd loop mutant constructs exhibit an approximate 50% loss in phosphorylation as compared with the wild-type receptor. These results suggest that at least one, or more, of the D_1 receptor phosphorylation sites resides within the 3rd cytoplasmic loop. Moreover, because the phosphorylation of the 3rd234 mutant was reduced to a similar extent as the 3rdTOT mutant, this suggests that the majority of the 3rd loop phosphorylation takes place on one or more of serine residues 256, 258, or 259. Notably, there is a glutamic acid residue (Glu-257) in close proximity to the three serine residues (Fig. 1) that would be predicted to enhance their phosphorylation by a GRK (1).

In order to assess the desensitization properties of the D_1 receptor with 3rd loop mutations, we expressed both the wild-type and 3rd234 receptor constructs in HEK293T cells, and we examined their ability to undergo agonist-induced desensitization. In the experiment shown in Fig. 6, each of the cell groups were pretreated with 10 μ_M dopamine for 1 h prior to constructing dopamine dose-response curves for stimulating cAMP accumulation. Comparison of Fig. 6*A* (WT) with Fig. 6*B* (3rd234) reveals that the mutant receptor exhibits attenuated desensitization properties. Average data for the wild-type and 3rd234 constructs are shown in Fig. 6*C*. Although the maximum response to dopamine is desensitized by about 40% by using this pretreatment paradigm, the 3rd234 response is only diminished by about 15%. Similar results were observed for the 3rdTOT construct (data not shown); however, it should be noted this construct exhibited altered potency for dopamine under basal conditions (Fig. 3). These results suggest that diminished phosphorylation of the 3rd234 mutant receptor is correlated with a diminished ability to undergo agonist-induced desensitization.

Phosphorylation and Desensitization of the Truncation Mutants

We next evaluated the ability of the D_1 receptor constructs with truncated carboxyl termini to undergo phosphorylation and desensitization. Fig. 7*A* shows the results from an *in situ* phosphorylation experiment using the wild-type and mutant receptor constructs. As can be seen, progressive truncation of the carboxyl terminus results in a progressive loss of both basal and dopamine-stimulated receptor phosphorylation until, surprisingly, no phosphorylation is observed with the most severely truncated receptor, T347. Average data from multiple experiments in which the phosphorylation data were quantified are shown in Fig. 7*B*.

In order to ensure that the data in Fig. 7 reflected a true loss of phosphorylation rather than a loss of receptor protein during SDS-PAGE, we performed intact cell biotinylation assays. Fig. 8 shows the results obtained from biotinylating the cell surface proteins in intact cells expressing the wild-type and truncated receptor constructs followed by solubilization, immunoprecipitation, and SDS-PAGE as performed in the experiment shown in Fig. 7. As

can be seen, equal amounts of receptor protein are present in the gels indicating that truncation of the D_1 receptor does not affect its ability to be processed in this manner.

We next assessed the ability of the truncated D_1 receptors to undergo agonist-induced desensitization. Fig. 9 shows dopamine dose-response curves for dopamine-stimulated cAMP accumulation, with and without agonist pretreatment, by using three of the truncated D_1 receptors. All three of these receptor constructs appear to desensitize in a similar fashion despite their variable phosphorylation response. After 1 h of dopamine pretreatment, there is an approximate 40% reduction in the maximum response to dopamine which is similar to that observed with the wild-type receptor (*cf.* Fig. 6). Fig. 10, *A* and *B*, shows a direct comparison between the wild-type receptor and phosphorylation-defective T347 mutant in response to agonist pretreatment. Surprisingly, both constructs appear to desensitize in an identical fashion. Average data from multiple desensitization experiments showing the cAMP response to a maximally effective dopamine concentration can be seen in Fig. 10*C*. There is no significant difference between the WT and T347 receptor constructs with each of them demonstrating an ~40% desensitization of the maximum response. These results suggest that the truncated T347 receptor is able to desensitize normally, even in the absence of its phosphorylation.

Given the results in Fig. 10, we were interested in determining whether mutation of the 3rd loop serines would attenuate agonist-induced desensitization if these mutations were created within the context of the truncated T347 construct. We thus created a T347/3rd234 construct in which serine residues 256, 258, and 259 (*cf.* Fig. 1) were mutated to alanines within the T347 D_1 receptor. Fig. 11 shows a desensitization experiment directly comparing the T347 (Fig. 11*A*) and T347/3rd234 (Fig. 11*B*) receptors. In this case, there does not appear to be any difference in the desensitization properties of the two receptor constructs. Fig. 11*C* provides a summary of the data shown in Figs. 6*C* and 10*C* and average data from the T347/3rd234 mutant. Clearly, simultaneous mutation of the 3rd loop serines 256, 258, and 259 only results in attenuation of agonist-induced desensitization when performed within the context of the wild-type receptor and not within the phosphorylation-defective T347 construct.

Assessment of Receptor-promoted Arrestin-GFP Translocation

Because we are interested in how phosphorylation of the D_1 receptor results in arrestin translocation and ultimately desensitization, we decided to examine the ability of arrestin proteins to interact with the various D_1 receptor constructs. Following the pioneering work by Caron and co-workers (20), we used GFP-tagged arrestin constructs in order to visualize their translocation from the cytosol to the plasma membrane in real time following receptor activation. Previously, it has been reported that the D_1 receptor interacts exclusively with arrestin3 (β-arrestin2) and is unable to promote the translocation of arrestin2 (β-arrestin1) to the plasma membrane (21, 22). We decided to first re-evaluate the differential interactions of the wild-type D_1 receptor with arrestin2 and arrestin3, and the results are shown in Fig. 12. Confocal fluorescence microscopy shows that both arrestin2-GFP and arrestin3-GFP are present in the cytosol under basal conditions (0 s). However, within 5 min (300 s) after the addition of dopamine to the media, both arrestin-GFP constructs are translocated from the

cytosol to the plasma membrane where they appear as punctate fluorescence clusters. Although the activation of the wild-type D_1 receptor was clearly able to promote the translocation of arrestin2, the plasma membrane-associated fluorescence following agonist treatment always appeared to be more intense using the arrestin3-GFP construct (Fig. 12). These results suggest that although arrestin2 and arrestin3 may exhibit differential interactions with the D_1 receptor, these differences may be more quantitative than qualitative in nature.

Fig. 13 shows a confocal microscopy experiment simultaneously using the WT receptor and the 3rd234 and T347 receptor constructs. In this case, we co-transfected the arrestin3-GFP construct with each receptor and examined their ability to promote arrestin3 translocation upon agonist activation. In comparison to the wild-type D_1 receptor, the 3rd234 mutant was clearly impaired in its ability to promote arrestin3-GFP translocation upon addition of dopamine to the media. In contrast, the T347 mutant receptor appeared to be comparable to the wild-type receptor with respect to arrestin3 translocation. Thus, the ability of the receptor constructs to promote arrestin translocation appears to be correlated with their ability to undergo agonist-induced desensitization (*cf*. Figs. 6 and 10).

DISCUSSION

Our current results have led us to propose the following model for D_1 receptor phosphorylation, arrestin association, and desensitization (Fig. 14). First, considering just the wild-type receptor, we propose that, under basal conditions, the carboxyl terminus (or parts thereof) is in close association with the 3rd cytoplasmic loop. Agonist occupancy of the receptor produces an altered confirmation allowing G protein coupling but also renders the receptor a substrate for GRK-mediated phosphorylation. We further propose that phosphorylation of the D_1 receptor takes place sequentially or in a hierarchical fashion, occurring first on residues within the carboxyl terminus and then within the 3rd cytoplasmic loop. Moreover, we believe that phosphorylation of the carboxyl terminus may be required for 3rd loop phosphorylation, perhaps by recruitment or orientation of the GRK. Finally, phosphorylation of the carboxyl terminus and the 3rd cytoplasmic loop promotes their dissociation, thereby allowing arrestin to bind to the activated 3rd cytoplasmic loop and disrupt G protein coupling. Key features of this model include the following: 1) arrestin does not bind to the carboxyl terminus as has been suggested for rhodopsin (4, 5) but rather binds to the 3rd cytoplasmic loop (although we cannot rule out additional interactions with the 1st and/or 2nd intracellular loops); 2) arrestin binding to the receptor is primarily driven by the activated conformation of the 3rd cytoplasmic loop; and 3) the role of receptor phosphorylation is to allow *access* of arrestin to its receptor binding domain rather than to create an arrestin binding site *per se*.

Consideration of this model can account for our experimental results currently obtained with the mutant D_1 receptors. With respect to the receptors containing serine mutations within the 3rd cytoplasmic loop, these constructs exhibit diminished phosphorylation within this domain with the receptor phosphorylation taking place primarily on the carboxyl terminus. Due to the diminished 3rd cytoplasmic loop phosphorylation, there is incomplete dissociation of this domain and the carboxyl terminus resulting in attenuated arrestin

translocation and desensitization (Fig. 14). With respect to the D_1 receptor constructs with truncations of the carboxyl terminus, phosphorylation is not required for desensitization as the steric hindrance of the carboxyl terminus is removed and arrestin binds rapidly to the activated receptor. This is particularly striking for the T347 mutant receptor which is phosphorylation-defective (Fig. 14). Indeed, within the context of this construct, further mutation of the 3rd cytoplasmic loop phosphorylation sites have no effect on its ability to undergo agonist-induced desensitization (Fig. 11). The fact that there is no observable phosphorylation with the T347 construct suggests that the carboxyl terminus is required for GRK-mediated phosphorylation of the 3rd cytoplasmic domain.

It is interesting to compare this model with that hypothesized for the β_2-adrenergic receptor as well as the desensitization kinetics of the two receptor systems. In the case of the β_2-adrenergic receptor, arrestin is believed to bind to phosphorylated segments of the carboxyl terminus of the receptor (6, 7). Agonist-induced desensitization of β_2-adrenergic receptor systems also occurs extremely rapidly (seconds to minutes) (1). In contrast, agonist-induced desensitization of D_1 receptor systems occurs relatively more slowly (minutes to hour) (Fig. 4). It is conceivable that the slower desensitization kinetics of the D_1 receptor is, at least partially, because of the steric requirements of arrestin association with the receptor.

An important aspect of our model is the association of the carboxyl terminus of the receptor with the 3rd cytoplasmic loop. Although there are currently no physicochemical data demonstrating this, Tiberi and co-workers (15, 23–25) have provided evidence consistent with the association of these two receptor domains. By using receptor chimeras and truncation mutants, these investigators have shown that the carboxyl termini of the D_1-like receptors (D_1 and D_5) play critical roles in determining agonist affinity, G protein coupling, and constitutive activity of the receptors (15, 23–25). Because it is unlikely that these functional effects are directly controlled by the carboxyl termini and it is known that the 3rd cytoplasmic loop is critical for D_1 receptor coupling to G_s (26) and also that the 3rd loop of the related D_3 receptor controls receptor affinity for agonists (27), the simplest explanation is the carboxyl terminus influences 3rd loop functions through direct domain-domain interactions.

Another interesting feature of the model is the proposed hierarchical nature of the receptor phosphorylation. Hierarchical phosphorylation of proteins, where phosphorylation of a primary site(s) is permissive for the phosphorylation of a secondary site(s), has been well described (28). This has not been extensively studied among GPCRs, although hierarchical phosphorylation by GRKs has been described previously for rhodopsin (29), *N*-formyl peptide (30), A_3 adenosine (31), and δ-opioid receptors (32). With the D_1 receptor, we are hypothesizing that primary phosphorylation of the carboxyl terminus is required for secondary phosphorylation of the 3rd cytoplasmic domain, and we are currently designing experiments to study the kinetics of these phosphorylation reactions in a site-specific fashion.

Our current results suggest the presence of functionally relevant phosphorylation sites in both the 3rd cytoplasmic loop as well as the carboxyl terminus of the D_1 receptor. Phosphorylation of both of these domains appears to be important for agonist-induced

arrestin association and desensitization. These results are in partial contrast with two recent reports (13, 15) suggesting that GRK-mediated phosphorylation sites are restricted to the carboxyl terminus of the D_1 receptor. In the study of Jackson *et al.* (15), this conclusion was inferred from experiments using receptors harboring only carboxyl-terminal mutations without direct mutational analysis of the 3rd cytoplasmic loop as performed in the present study. In contrast, Lamey *et al.* (13) showed that a D_1 receptor with mutations in all of the 3rd cytoplasmic loop serines and threonines underwent agonist-induced desensitization in a normal fashion. This group found that only a single threonine residue (T360) in the carboxyl terminus was required for agonist-induced phosphorylation and desensitization. It is not completely clear what accounts for the difference between our results and those of Lamey *et al.* (13), although one possibility is that their investigation was conducted with the human D_1 receptor and ours was performed using the rat receptor. Another more likely explanation is that Lamey *et al.* (13) used CHO cells for receptor expression, and we used HEK293 cells. We have shown previously that the rate of agonist-induced desensitization of the D_1 receptor in CHO occurs more slowly than in other cell types (33), suggesting that CHO cells may lack an important component of desensitization. One intriguing possibility is that the 3rd cytoplasmic loop and the carboxyl terminus of the D_1 receptor may undergo differential phosphorylation by separate GRK isoforms, and one of these is lacking in CHO cells. Indeed, GRKs 2–5 have all been shown to be capable of phosphorylating and desensitizing the D_1 receptor in various cell systems (10, 34). It will be important in future studies to examine the effects of overexpressing each of these GRKs with the D_1 receptor constructs used in this study as well as to delineate the specific GRK sites involved.

Our present results may have general applicability to many other GPCR systems. Recently, Ascoli and co-workers (35) have reported that the association of arrestin3 with the human lutropin receptor depends mostly on receptor activation rather than on receptor phosphorylation. Similarly, this group has shown that a segment of the carboxyl terminus of the rat follitropin receptor modulates arrestin3 binding to intracellular loops of the receptor protein in a phosphorylation-independent fashion (36). In addition, Murray *et al.* (37) have shown that truncation of the carboxyl terminus of the δ opioid receptor results in a phosphorylation-defective receptor, yet this construct still undergoes agonist-induced, dynamin-dependent internalization. Finally, Richardson *et al.* (38) have shown that a substance P receptor lacking the C-terminal domain remains competent to desensitize and internalize. These recent results derived from diverse types of GPCRs suggest that the model proposed in Fig. 14 may have widespread applicability, particularly for GPCRs that associate with arrestin proteins via their intracellular loops.

Supplementary Material

Refer to Web version on PubMed Central for supplementary material.

REFERENCES

1. Ferguson SS. Pharmacol. Rev. 2001; 53:1–24. [PubMed: 11171937]
2. Pierce KL, Lefkowitz RJ. Nat. Rev. Neurosci. 2001; 2:727–733. [PubMed: 11584310]
3. Kohout TA, Lefkowitz RJ. Mol. Pharmacol. 2003; 63:9–18. [PubMed: 12488531]

4. Vishnivetskiy SA, Paz CL, Schubert C, Hirsch JA, Sigler PB, Gurevich VV. J. Biol. Chem. 1999; 274:11451–11454. [PubMed: 10206946]
5. Vishnivetskiy SA, Schubert C, Climaco GC, Gurevich YV, Velez MG, Gurevich VV. J. Biol. Chem. 2000; 275:41049–41057. [PubMed: 11024026]
6. Kovoor A, Celver J, Abdryashitov RI, Chavkin C, Gurevich VV. J. Biol. Chem. 1999; 274:6831–6834. [PubMed: 10066734]
7. Celver J, Vishnivetskiy SA, Chavkin C, Gurevich VV. J. Biol. Chem. 2002; 277:9043–9048. [PubMed: 11782458]
8. Sibley, DR.; Neve, KA. The Dopamine Receptors. Neve, KA.; Neve, RL., editors. Totowa, NJ: Humana Press Inc; 1996. p. 383-424.
9. Mason JN, Kozell LB, Neve KA. Mol. Pharmacol. 2002; 61:806–816. [PubMed: 11901220]
10. Tiberi M, Nash SR, Bertrand L, Lefkowitz RJ, Caron MG. J. Biol. Chem. 1996; 271:3771–3778. [PubMed: 8631993]
11. Lewis MM, Watts VJ, Lawler CP, Nichols DE, Mailman RB. J. Pharmacol. Exp. Ther. 1998; 286:345–353. [PubMed: 9655879]
12. Gardner B, Liu ZF, Jiang D, Sibley DR. Mol. Pharmacol. 2001; 59:310–321. [PubMed: 11160868]
13. Lamey M, Thompson M, Varghese G, Chi H, Sawzdargo M, George SR, O'Dowd BF. J. Biol. Chem. 2002; 277:9415–9421. [PubMed: 11773080]
14. Jiang D, Sibley DR. Mol. Pharmacol. 1999; 56:675–683. [PubMed: 10496949]
15. Jackson A, Iwasiow RM, Chaar ZY, Nantel MF, Tiberi M. J. Neurochem. 2002; 82:683–697. [PubMed: 12153492]
16. Heinzel SS, Krysan PJ, Calos MP, DuBridge RB. J. Virol. 1988; 62:3738–3746. [PubMed: 2843671]
17. Monsma FJ Jr, Mahan LC, McVittie LD, Gerfen CR, Sibley DR. Proc. Natl. Acad. Sci. U. S. A. 1990; 87:6723–6727. [PubMed: 2168556]
18. Guan XM, Kobilka TS, Kobilka BK. J. Biol. Chem. 1992; 267:21995–21998. [PubMed: 1331042]
19. Kim KM, Valenzano KJ, Robinson SR, Yao WD, Barak LS, Caron MG. J. Biol. Chem. 2001; 276:37409–37414. [PubMed: 11473130]
20. Barak LS, Zhang J, Ferguson SSG, Laporte SA, Caron MG. Methods Enzymol. 1999; 302:153–171. [PubMed: 12876769]
21. Zhang J, Barak LS, Anborgh PH, Laporte SA, Caron MG, Ferguson SS. J. Biol. Chem. 1999; 274:10999–11006. [PubMed: 10196181]
22. Oakley RH, Laporte SA, Holt JA, Caron MG, Barak LS. J. Biol. Chem. 2000; 275:17201–17210. [PubMed: 10748214]
23. Jackson A, Iwasiow RM, Tiberi M. FEBS Lett. 2000; 470:183–188. [PubMed: 10734231]
24. Chaar ZY, Jackson A, Tiberi M. J. Neurochem. 2001; 79:1047–1058. [PubMed: 11739618]
25. Tumova K, Iwasiow RM, Tiberi M. J. Biol. Chem. 2003; 278:8146–8153. [PubMed: 12509438]
26. Kozell LB, Machida CA, Neve RL, Neve KA. J. Biol. Chem. 1994; 269:30299–30306. [PubMed: 7982941]
27. Robinson SW, Jarvie KR, Caron MG. Mol. Pharmacol. 1994; 46:352–356. [PubMed: 7915820]
28. Roach PJ. J. Biol. Chem. 1991; 266:14139–14142. [PubMed: 1650349]
29. Ohguro H, Palczewski K, Ericsson LH, Walsh KA, Johnson RS. Biochemistry. 1993; 32:5718–5724. [PubMed: 8504090]
30. Prossnitz ER, Kim CM, Benovic JL, Ye RD. J. Biol. Chem. 1995; 270:1130–1137. [PubMed: 7836371]
31. Palmer TM, Stiles GL. Mol. Pharmacol. 2000; 57:539–545. [PubMed: 10692494]
32. Kouhen OM, Wang G, Solberg J, Erickson LJ, Law PY, Loh HH. J. Biol. Chem. 2000; 275:36659–36664. [PubMed: 10973976]
33. Ventura AL, Sibley DR. J. Pharmacol. Exp. Ther. 2000; 293:426–434. [PubMed: 10773012]
34. Felder RA, Sanada H, Xu J, Yu PY, Wang Z, Watanabe H, Asico LD, Wang W, Zheng S, Yamaguchi I, Williams SM, Gainer J, Brown NJ, Hazen-Martin D, Wong LJ, Robillard JE, Carey

RM, Eisner GM, Jose PA. Proc. Natl. Acad. Sci. U. S. A. 2002; 99:3872–3877. [PubMed: 11904438]

35. Min L, Galet C, Ascoli M. J. Biol. Chem. 2002; 277:702–710. [PubMed: 11696538]
36. Kishi H, Krishnamurthy H, Galet C, Bhaskaran RS, Ascoli M. J. Biol. Chem. 2002; 277:21939–21946. [PubMed: 11934883]
37. Murray SR, Evans CJ, von Zastrow M. J. Biol. Chem. 1998; 273:24987–24991. [PubMed: 9737953]
38. Richardson MD, Balius AM, Yamaguchi K, Freilich ER, Barak LS, Kwatra MM. J. Neurochem. 2003; 84:854–863. [PubMed: 12562528]

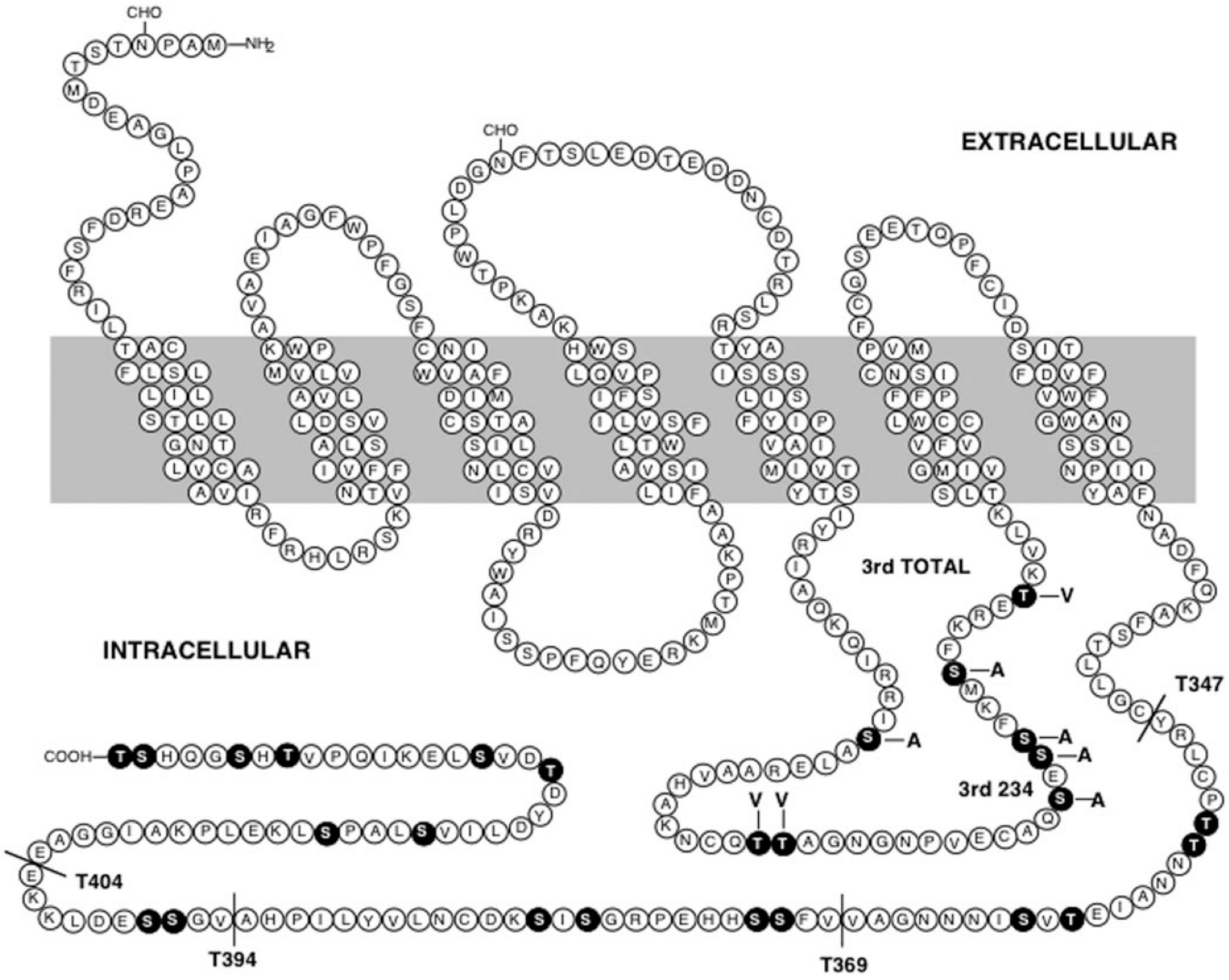

Fig. 1. Diagram of the rat D_1 dopamine receptor sequence

The wild-type (*WT*) receptor sequence is shown along with the various mutant constructs utilized in this study. The *black residues* highlight the serine and threonine residues within the 3rd cytoplasmic loop and carboxyl-terminal domains. Four truncation mutants are shown (T347, T369, T394, and T404) in which the receptor was truncated at the position indicated. Two 3rd loop mutants are shown. In the 3rd TOTAL (*3rdTOT*) mutant, all of the serine and threonine residues within the 3rd cytoplasmic loop were changed to either alanine or valine as indicated. In the 3rd234 mutant, only the three serine residues indicated (serines 256, 258, and 259) were mutated to alanines.

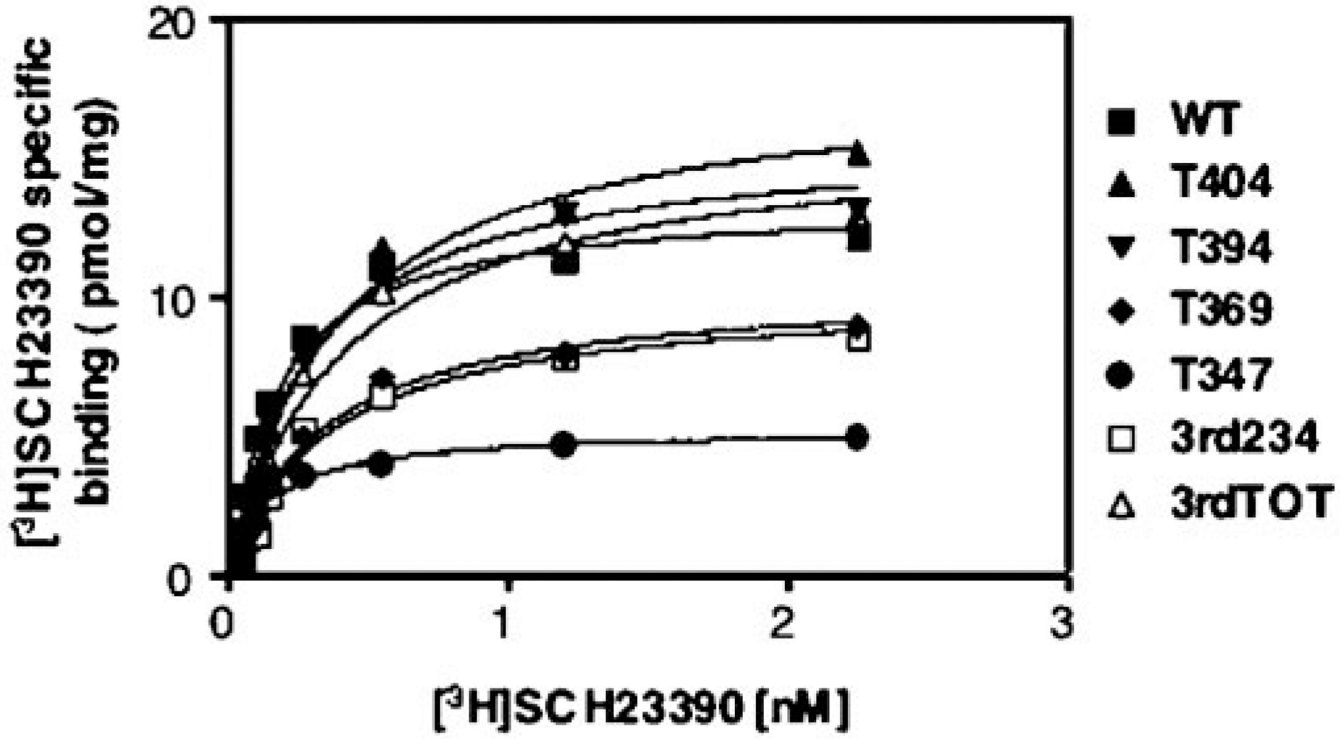

Fig. 2. Expression of wild-type and mutant D_1 receptors in HEK293T cells

The D_1 receptor constructs were transiently transfected into HEK293T cells as described under "Experimental Procedures." The cells were harvested, membranes prepared, and [^{3}H]SCH-23390 saturation binding assays performed as described under "Experimental Procedures." The lines were drawn using non-linear regression analysis with the GraphPad PRIZM software package. The WT receptor exhibited a K_D of 0.25 nM for [^{3}H]SCH23390, and this did not differ significantly for any of the mutant receptors. A single experiment, representative of three, is shown.

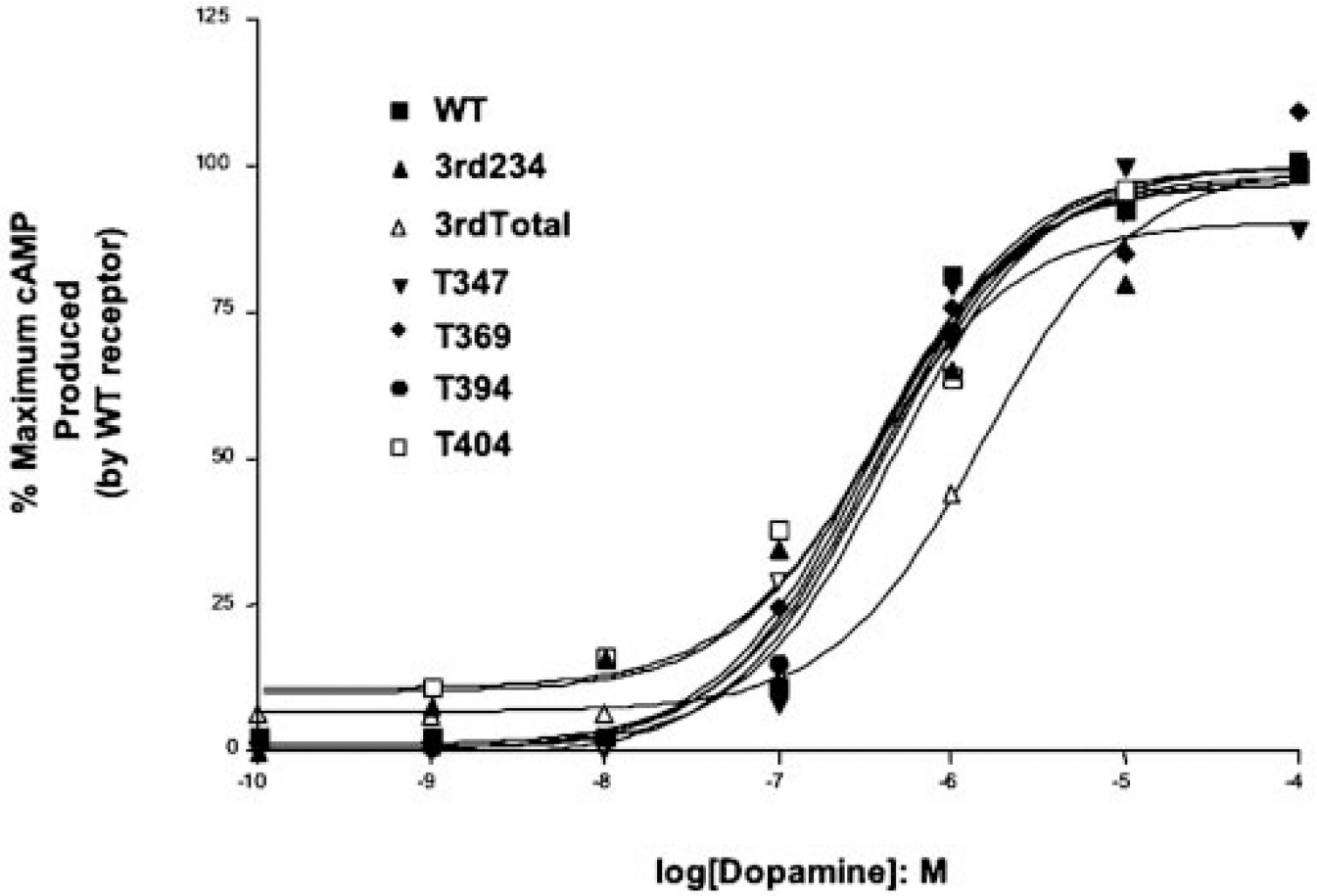

Fig. 3. Accumulation of cAMP in HEK293T cells transfected with WT and mutant D_1 dopamine receptors

The D_1 receptor constructs were transiently transfected into HEK293T cells and used 2 days later for the cAMP accumulation experiments as described under "Experimental Procedures." The data are expressed as a percentage of the maximum cAMP response produced by the WT receptor. All of the constructs exhibited a similar potency for dopamine (EC_{50} = 300 nM) except for the 3rdTOT mutant which consistently showed a 3–4-fold rightward shift in the dose-response curve (EC_{50} = 1.1 μM). A single experiment, representative of three, is shown.

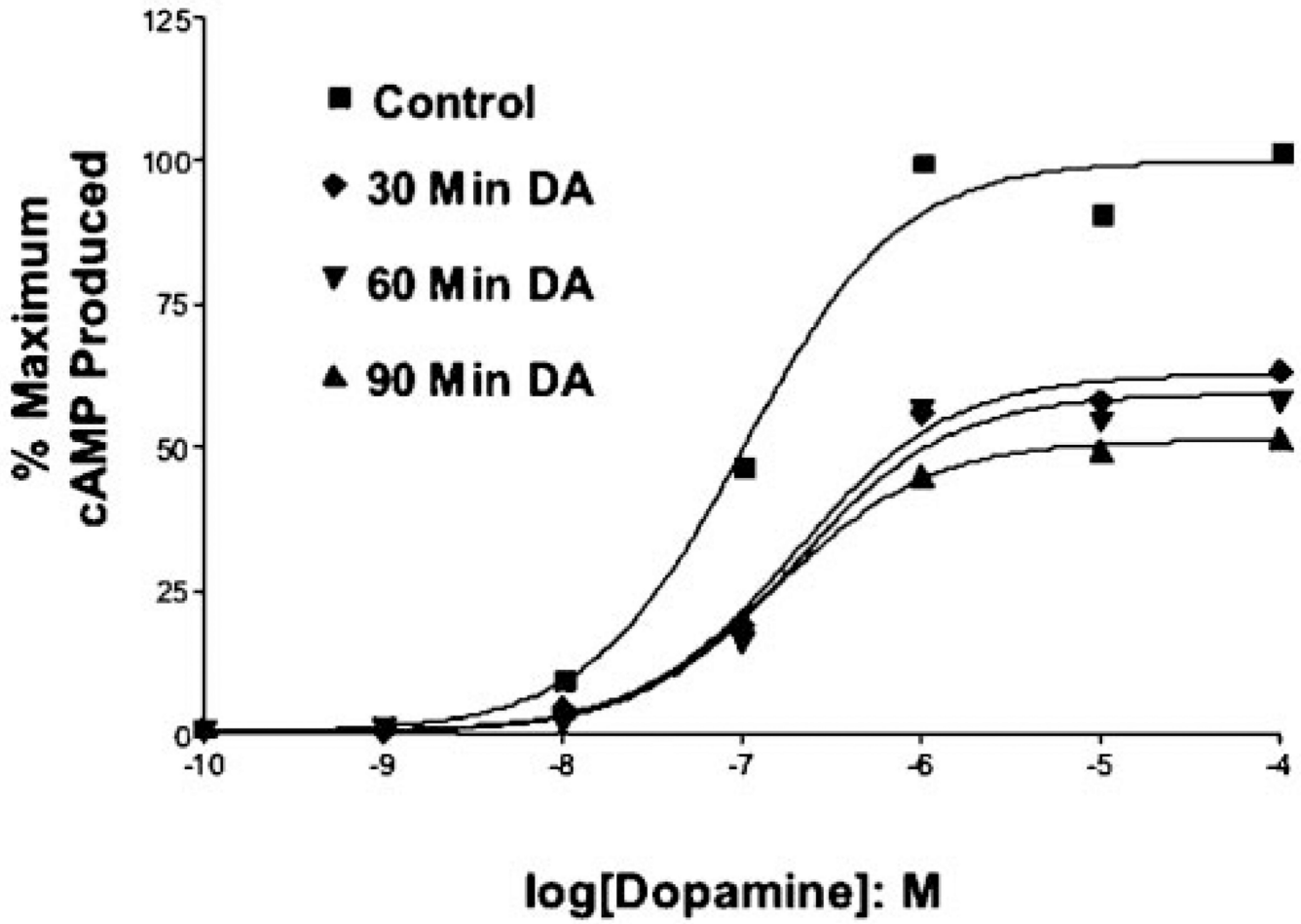

Fig. 4. Agonist-induced desensitization of the wild-type D_1 receptor in HEK293T cells

Transiently transfected HEK293T cells were pretreated with 0.01 mM dopamine (*DA*) for the indicated times, washed, and then re-challenged with the indicated doses of dopamine. The data are expressed as a percentage of the maximum cAMP response produced by the control group that was not pretreated with dopamine. A single experiment, representative of three, is shown. In this experiment, the EC_{50} values for dopamine in the cell treatment groups are as follows: control, 0.1 μM; 30 min, 0.15 μM; 60 min, 0.2 μM; and 90 min, 0.2 μM.

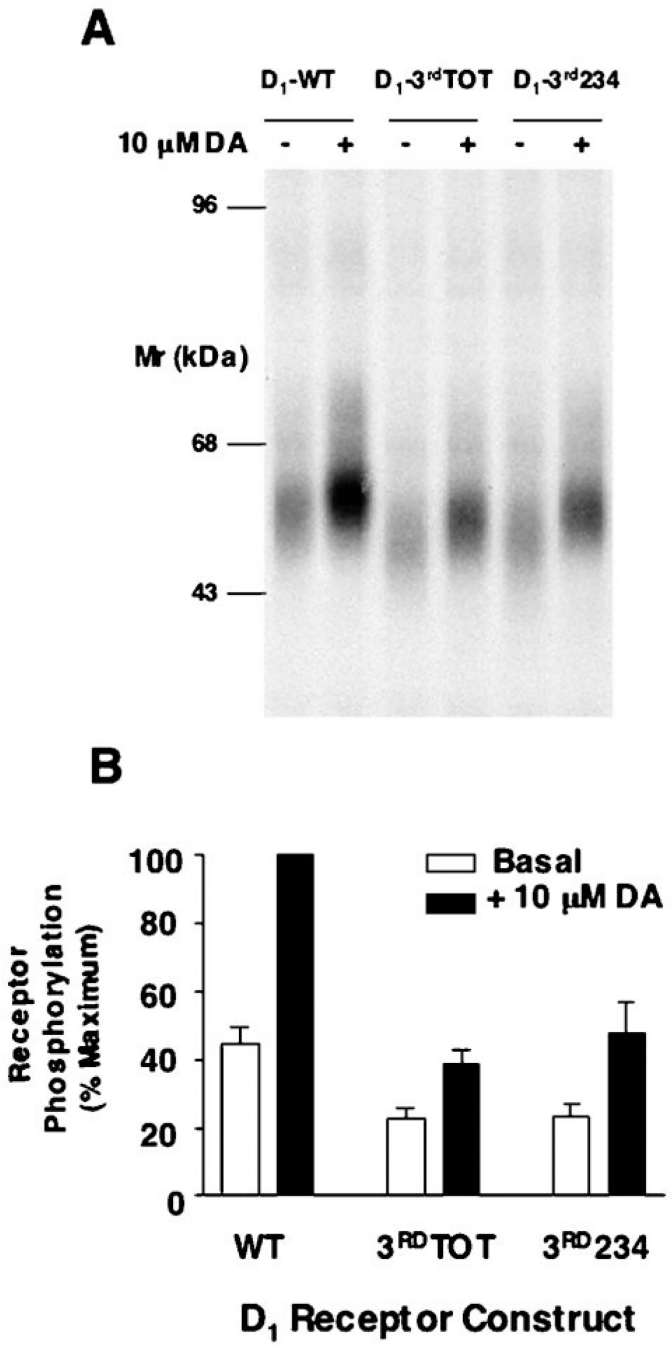

Fig. 5. Agonist-induced phosphorylation of the WT and 3rd loop mutant D_1 receptors

A, autoradiogram of SDS-PAGE analysis of immunoprecipitates from whole cell phosphorylation assays. HEK293T cells were transiently transfected with the WT and 3rdTOT and 3rd234 receptor constructs, pre-labeled with $[^{32}P]H_3PO_4$, and treated with vehicle (basal) or 10 μM dopamine (*DA*) for 10 min. Samples were then subjected to immunoprecipitation as described under "Experimental Procedures" and resolved by 8% SDS-PAGE. Receptors were quantified, and equal amounts of receptor protein were loaded into each gel lane as described under "Experimental Procedures." A representative

experiment is shown. *B*, the receptor phosphorylation was quantified by scanning the autographs followed by analysis with the software package NIH Image. Data are the mean values (±S.E.) of band density (arbitrary units) from 3 independent experiments and are presented as a percentage of the maximum phosphorylation observed (WT + 10 μM dopamine).

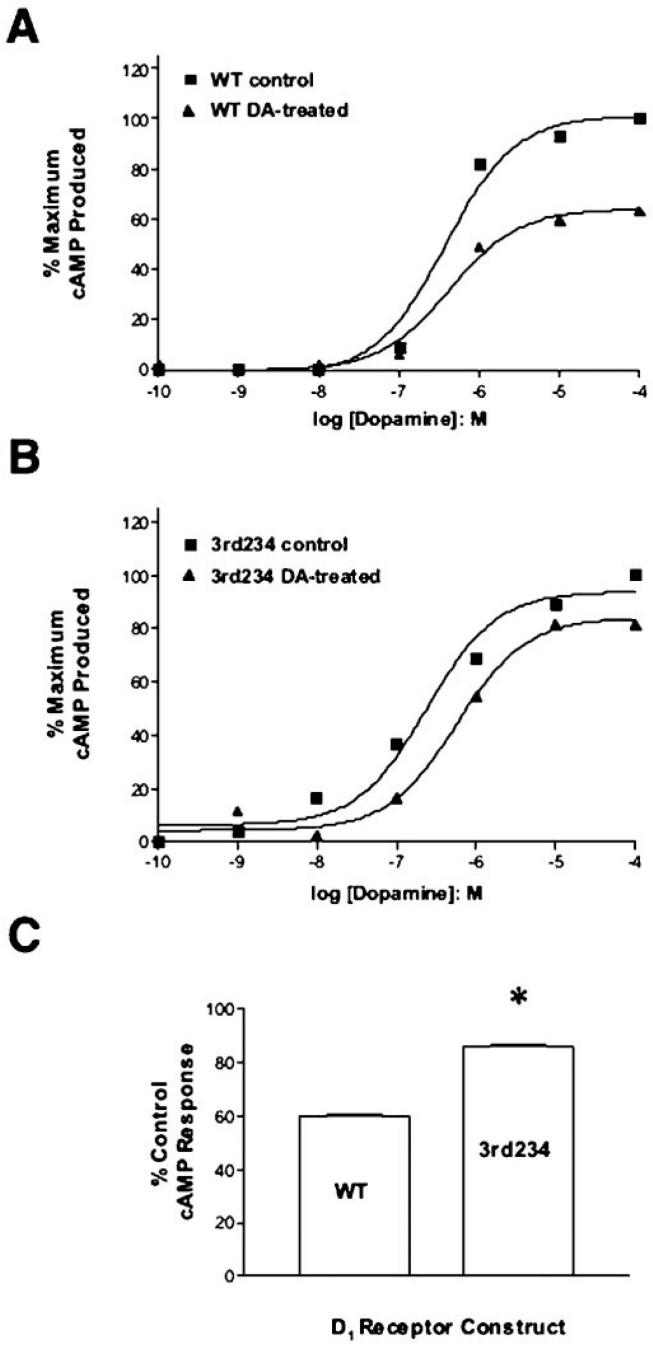

Fig. 6. Agonist-induced desensitization of the WT and 3rd234 mutant D_1 receptors

Transiently transfected HEK293T cells were pretreated with 0.01 mM dopamine for 1 h, washed, and then rechallenged with the indicated doses of dopamine. The data are expressed as a percentage of the maximum cAMP response produced by the control group that was not pretreated with dopamine (*DA*). *A*, a single experiment, representative of three, is shown for the WT receptor. *B*, a single experiment, representative of three, is shown for the 3rd234 receptor. *C*, average data from three separate experiments performed as described in *A* and *B* are shown. The data represent the maximum cAMP response to 100 μM dopamine, after 1 h

of dopamine pretreatment (10 μM), expressed a percentage of the control group. Mean ± S.E. values are shown. The *asterisk* indicates that the 3rd234 mutant values are significantly different from the wild-type receptor values (Student's *t* test, $p < 0.05$).

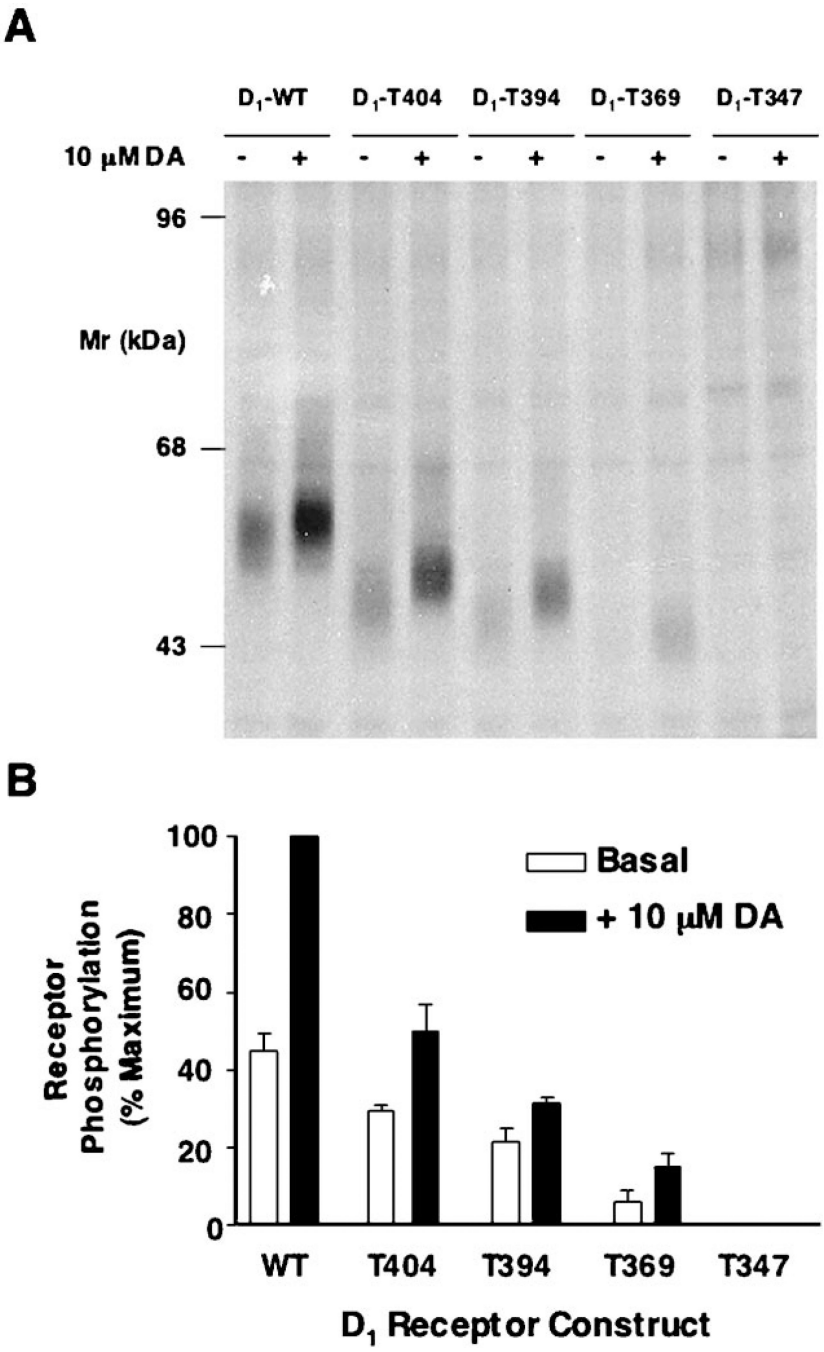

Fig. 7. Agonist-induced phosphorylation of the WT and truncated D_1 receptors

A, autoradiogram of SDS-PAGE analysis of immunoprecipitates from whole cell phosphorylation assays. HEK293T cells were transiently transfected with the WT and truncation receptor constructs, pre-labeled with $[^{32}P]H_3PO_4$, and treated with vehicle (basal) or 10 μM dopamine (*DA*) for 10 min. Samples were then subjected to immunoprecipitation as described under "Experimental Procedures" and resolved by 8% SDS-PAGE. Receptors were quantified, and equal amounts of receptor protein were loaded into each gel lane as described under "Experimental Procedures." A representative experiment is shown. *B*, the

receptor phosphorylation was quantified by scanning the autographs followed by analysis with the software package NIH Image. Data are the mean values (±S.E.) of band density (arbitrary units) from three independent experiments and are presented as a percentage of the maximum phosphorylation observed (WT + 10 μM dopamine).

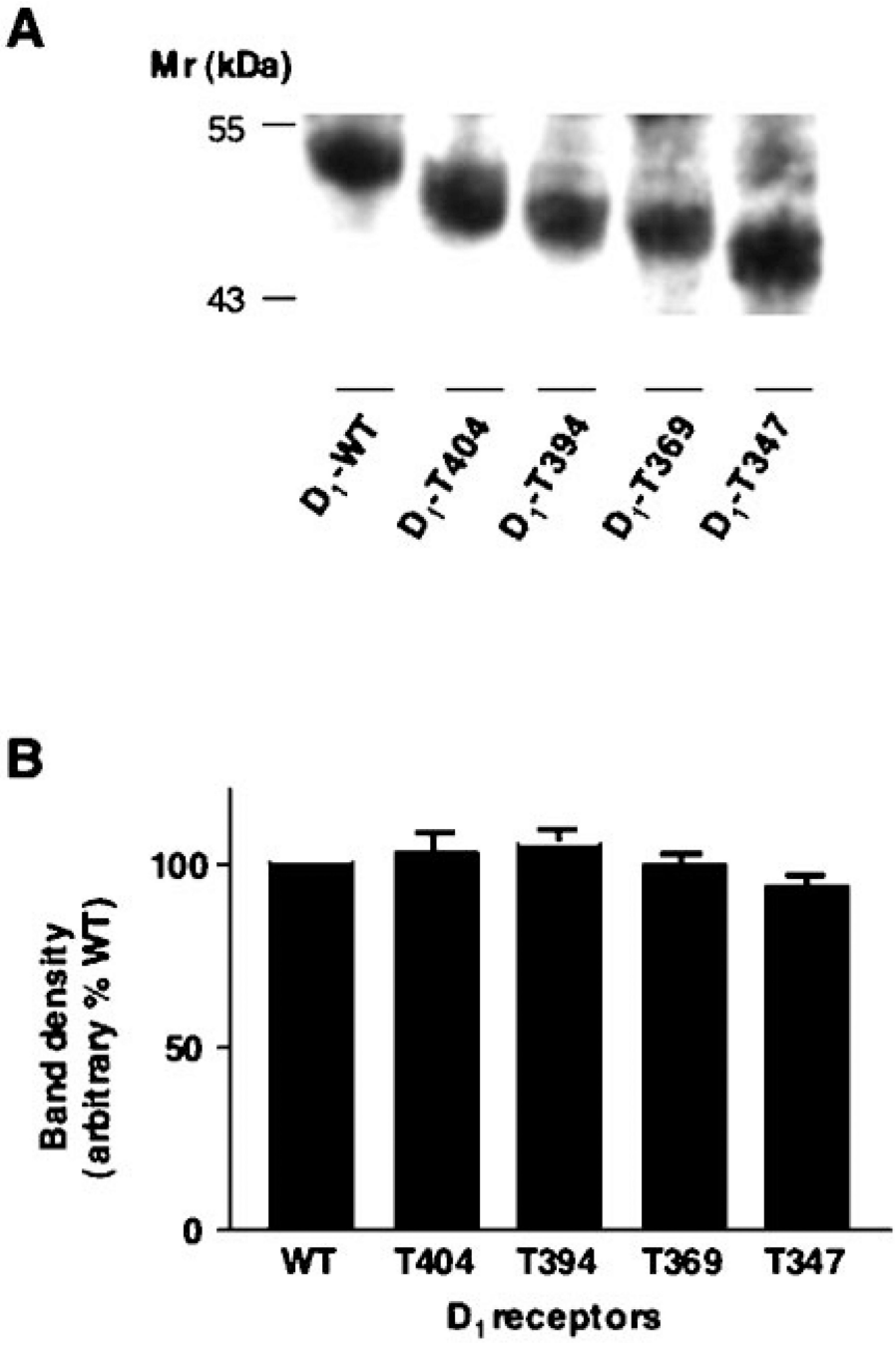

Fig. 8. Cell surface biotinylation of the WT and truncated D_1 receptor constructs expressed in HEK293T cells

The indicated receptor constructs were transiently expressed in HEK293T cells and subjected to cell surface biotinylation. The cells were then solubilized, and the receptors were immunoprecipitated as performed for the experiment shown in Fig. 7. Receptors were quantified, and equal amounts of receptor protein were loaded into each gel lane as described under "Experimental Procedures." *A*, SDS-PAGE of a representative experiment is shown. *B*, the biotinylated proteins were quantified by densitometry as described under

"Experimental Procedures." The data are expressed as a percentage of the WT sample. Average data from three separate experiments are shown (mean ± S.E.).

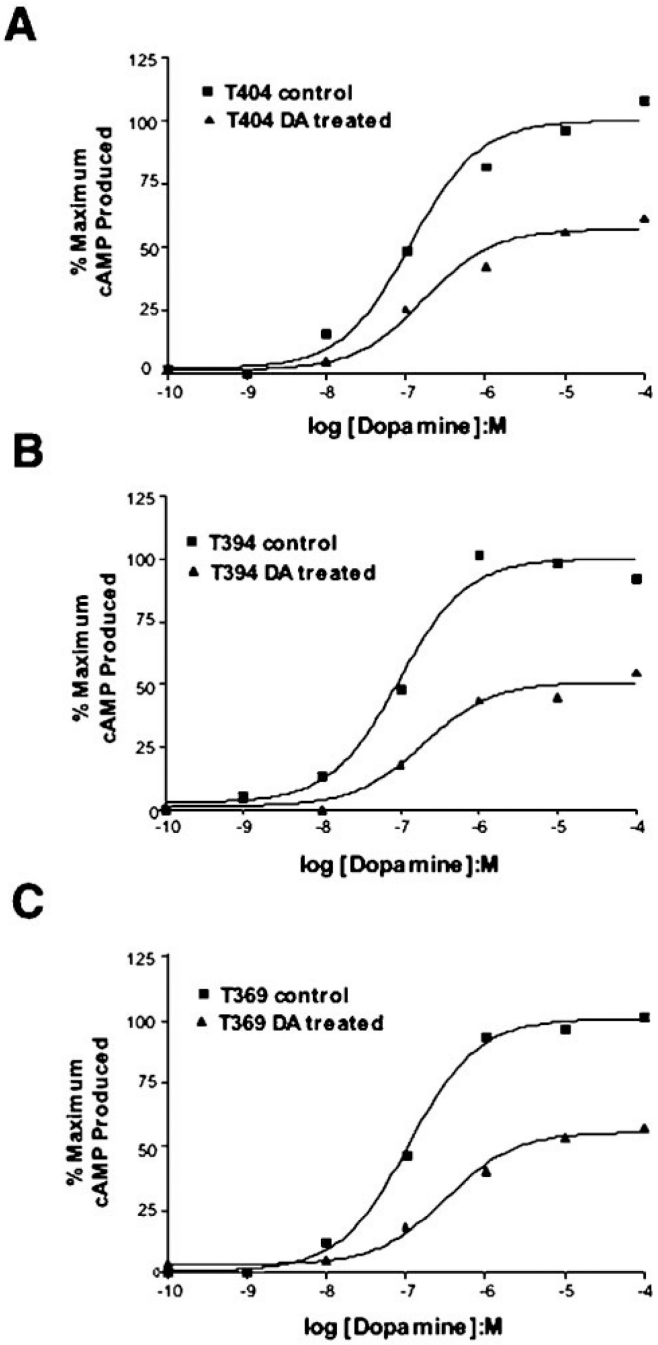

Fig. 9. Agonist-induced desensitization of partially truncated D_1 receptors

Transiently transfected HEK293T cells were pretreated with 10 μM dopamine (*DA*) for 1 h, washed, and then re-challenged with the indicated doses of dopamine. The data are expressed as a percentage of the maximum cAMP response produced by the control group that was not pretreated with dopamine. *A*, a single experiment, representative of three, is shown for the T404 receptor. *B*, a single experiment, representative of three, is shown for the T394 receptor. *C*, a single experiment, representative of three, is shown for the T369 receptor.

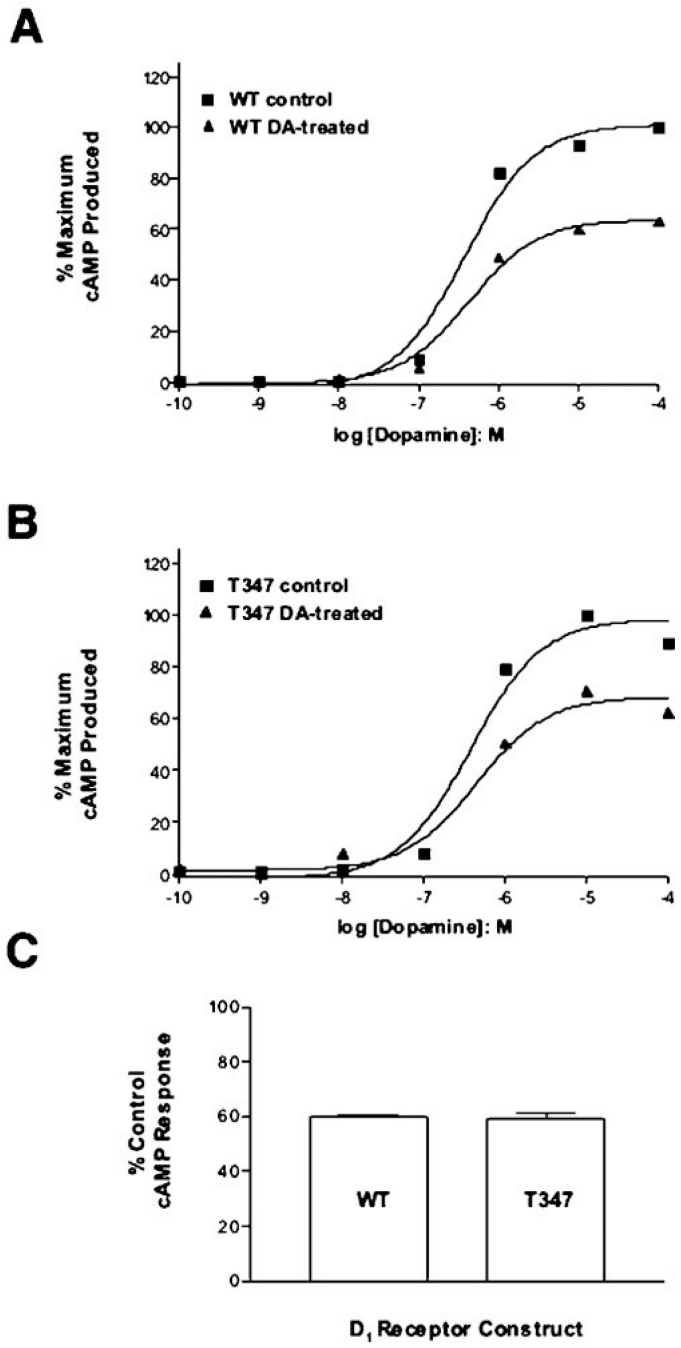

Fig. 10. Agonist-induced desensitization of the WT and T347 mutant D_1 receptors

Transiently transfected HEK293T cells were pretreated with 10 μM dopamine (*DA*) for 1 h, washed, and then rechallenged with the indicated doses of dopamine. The data are expressed as a percentage of the maximum cAMP response produced by the control group that was not pretreated with dopamine. *A*, a single experiment, representative of three, is shown for the WT receptor. *B*, a single experiment, representative of three, is shown for the T347 receptor. *C*, average data from three separate experiments performed as described in *A* and *B* are shown. The data represent the maximum cAMP response to 100 μM dopamine, after 1 h of

dopamine pretreatment (10 μM), expressed a percentage of the control group in each experiment. Mean ± S.E. values are shown.

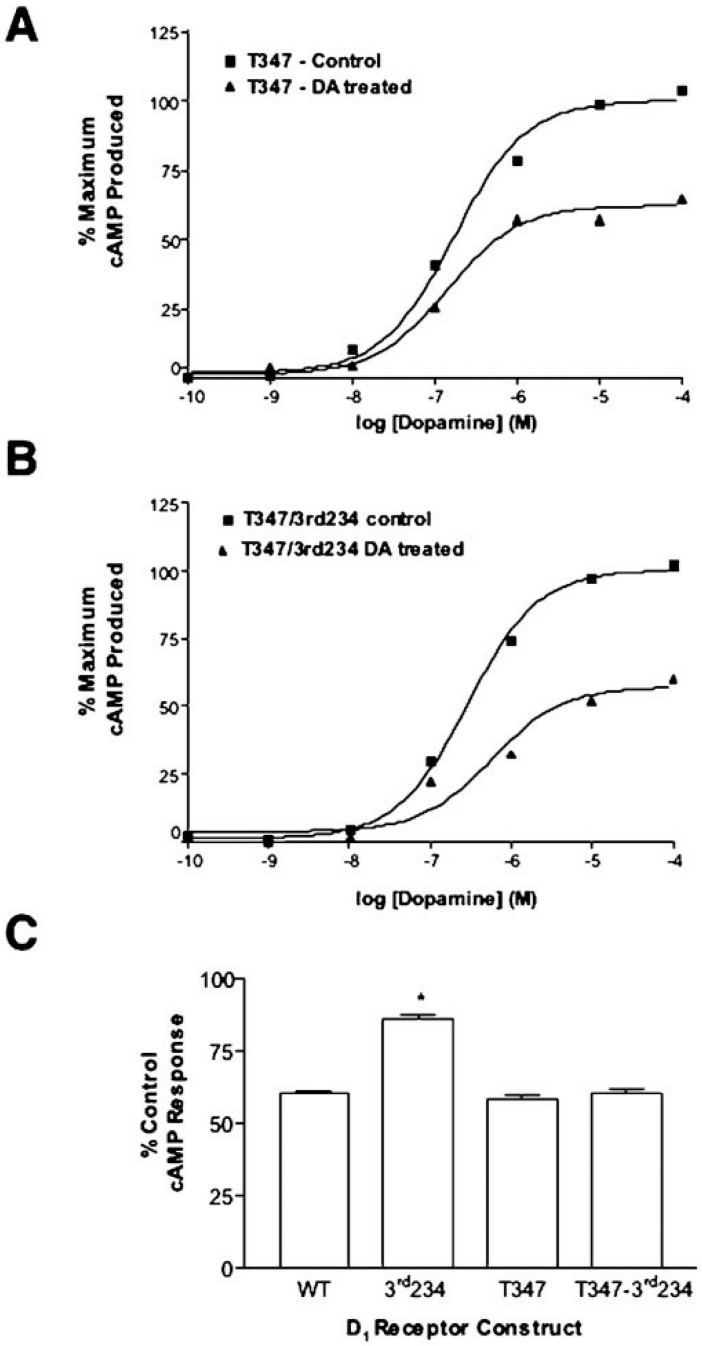

Fig. 11. Agonist-induced desensitization of the T347 and T347/3rd234 mutant D_1 receptors

Transiently transfected HEK293T cells were pretreated with 10 μM dopamine (*DA*) for 1 h, washed, and then re-challenged with the indicated doses of dopamine. The data are expressed as a percentage of the maximum cAMP response produced by the control group that was not pretreated with dopamine. *A*, a single experiment, representative of three, is shown for the T347 receptor. *B*, a single experiment, representative of three, is shown for the T347/3rd234 receptor. *C*, average data (mean ± S.E. values) from three separate experiments using the indicated constructs. The data represent the maximum cAMP response to 100 μM

dopamine, after 1 h of dopamine (10 μM) pretreatment, expressed a percentage of the control group in each experiment. For comparison purposes, data from Figs. 6*C* and 10*C* are included.

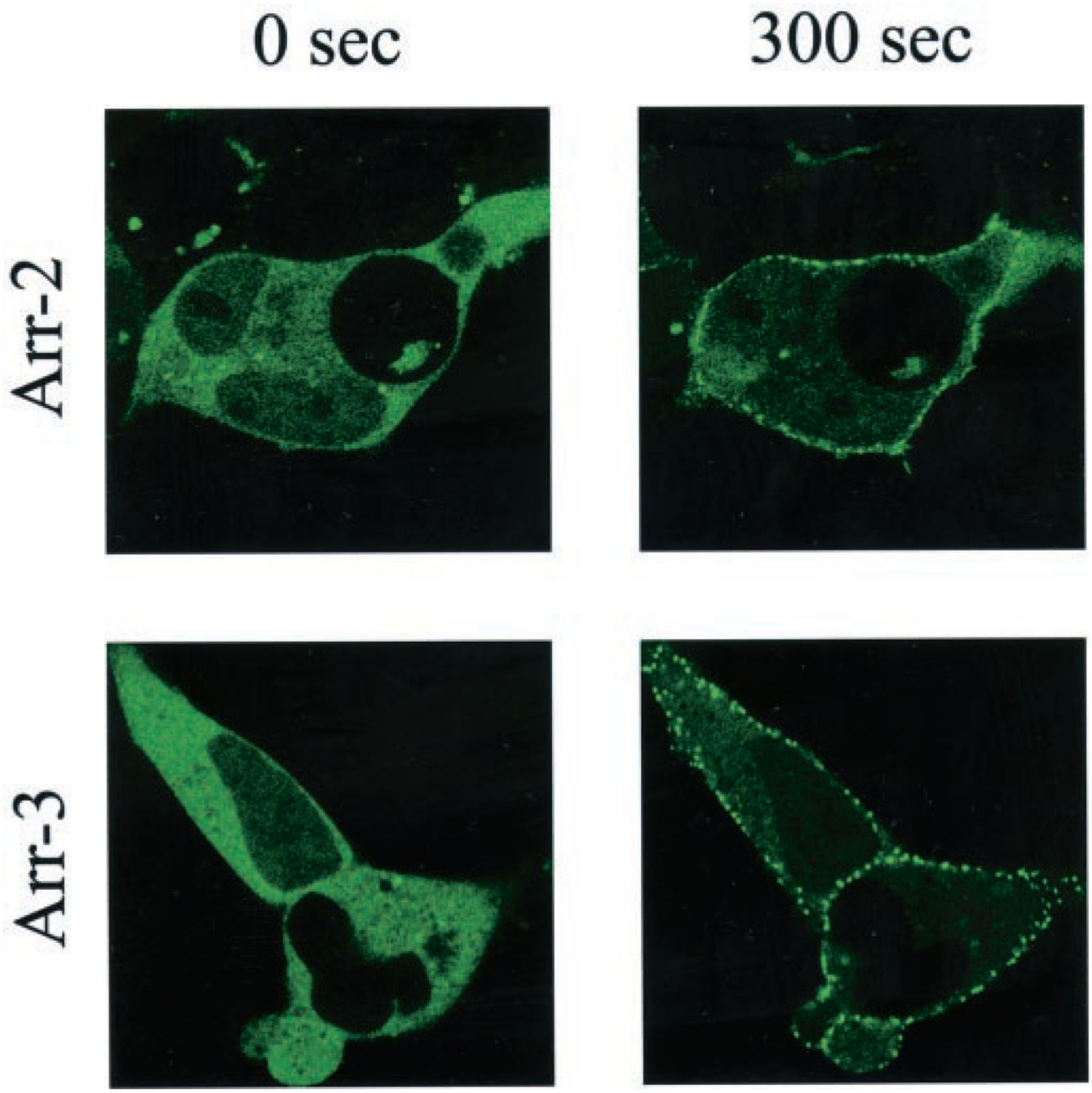

Fig. 12. Translocation of arrestin2-GFP and arrestin3-GFP to the wild-type D_1 receptor

HEK293 cells were transiently transfected with the wild-type D_1 receptor and either arrestin2-GFP or arrestin3-GFP. Twenty-four hours post-transfection, cells were plated on 35-mm glass bottom culture dishes, and confocal microscopy was performed on a Zeiss laser-scanning confocal microscope (LSM-510). Images were collected sequentially every 30 s after agonist stimulation with 20 μM dopamine using single line excitation (488 nm). Shown are representative confocal microscopic images of arrestin2-GFP or arrestin3-GFP fluorescence 300 s (5 min) after treatment with dopamine. Movies showing the dopamine

treatments from 0 to 20 min are provided as Supplemental Material for the arrestin2-GFP and arrestin3-GFP constructs. This experiment was performed three times with similar results.

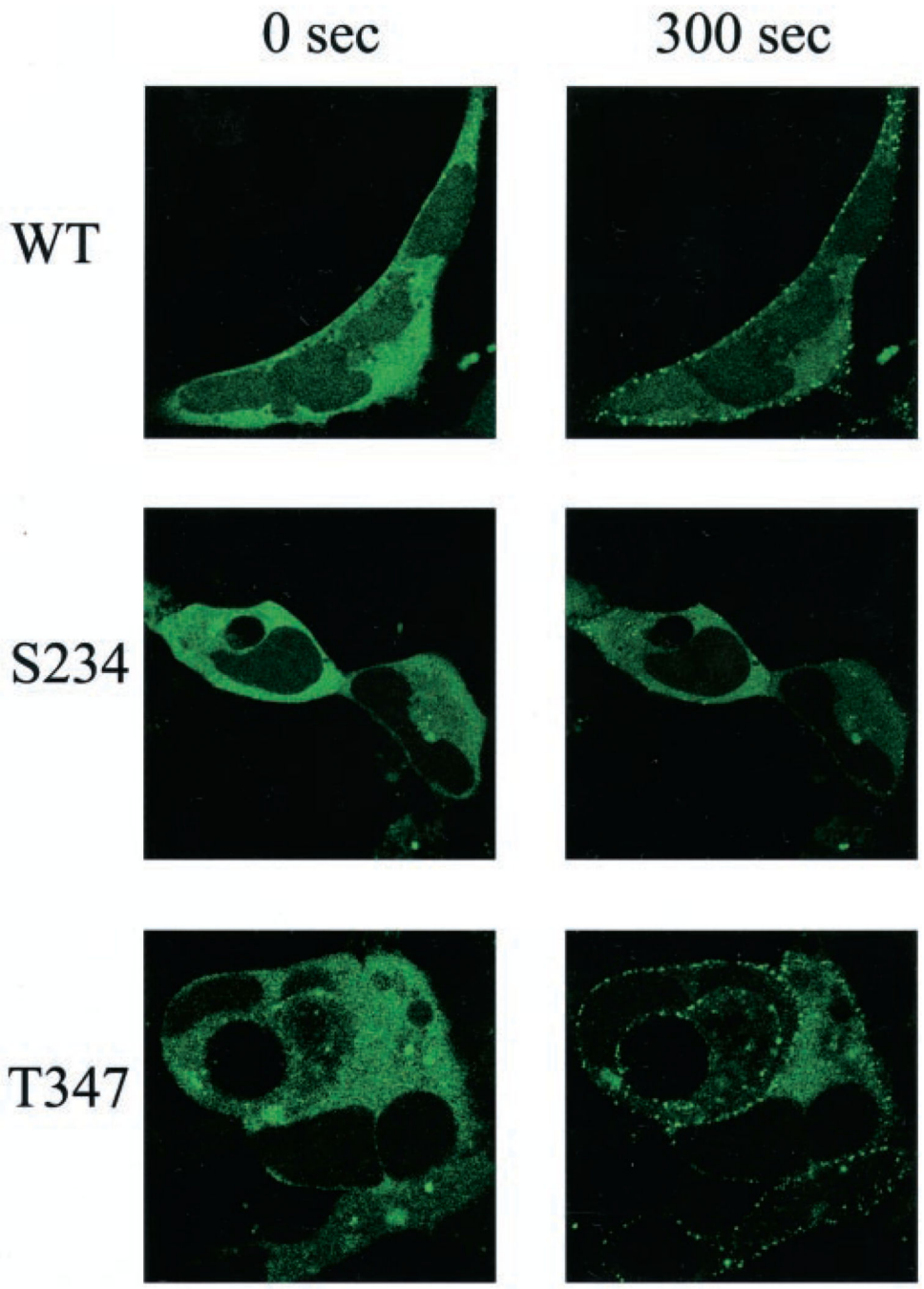

Fig. 13. Translocation of arrestin3-GFP to the wild-type and mutant D_1 receptors

HEK293 cells were transiently transfected with arrestin3-GFP and either the WT, Ser-234 or T347 D_1 receptor constructs. Twenty four hours post-transfection, cells were plated on 35-mm glass-bottom culture dishes, and confocal microscopy was performed on a Zeiss laser-scanning confocal microscope (LSM-510). Images were collected sequentially every 30 s after agonist stimulation with 20 μM dopamine using single line excitation (488 nm). Shown are representative confocal microscopic images of arrestin3-GFP fluorescence 300 s (5 min) after treatment with dopamine. Movies showing the dopamine treatments from 0 to 20 min

are provided as Supplemental Material for the WT, Ser-234, and T347 D_1 receptor constructs. This experiment was performed three times with similar results.

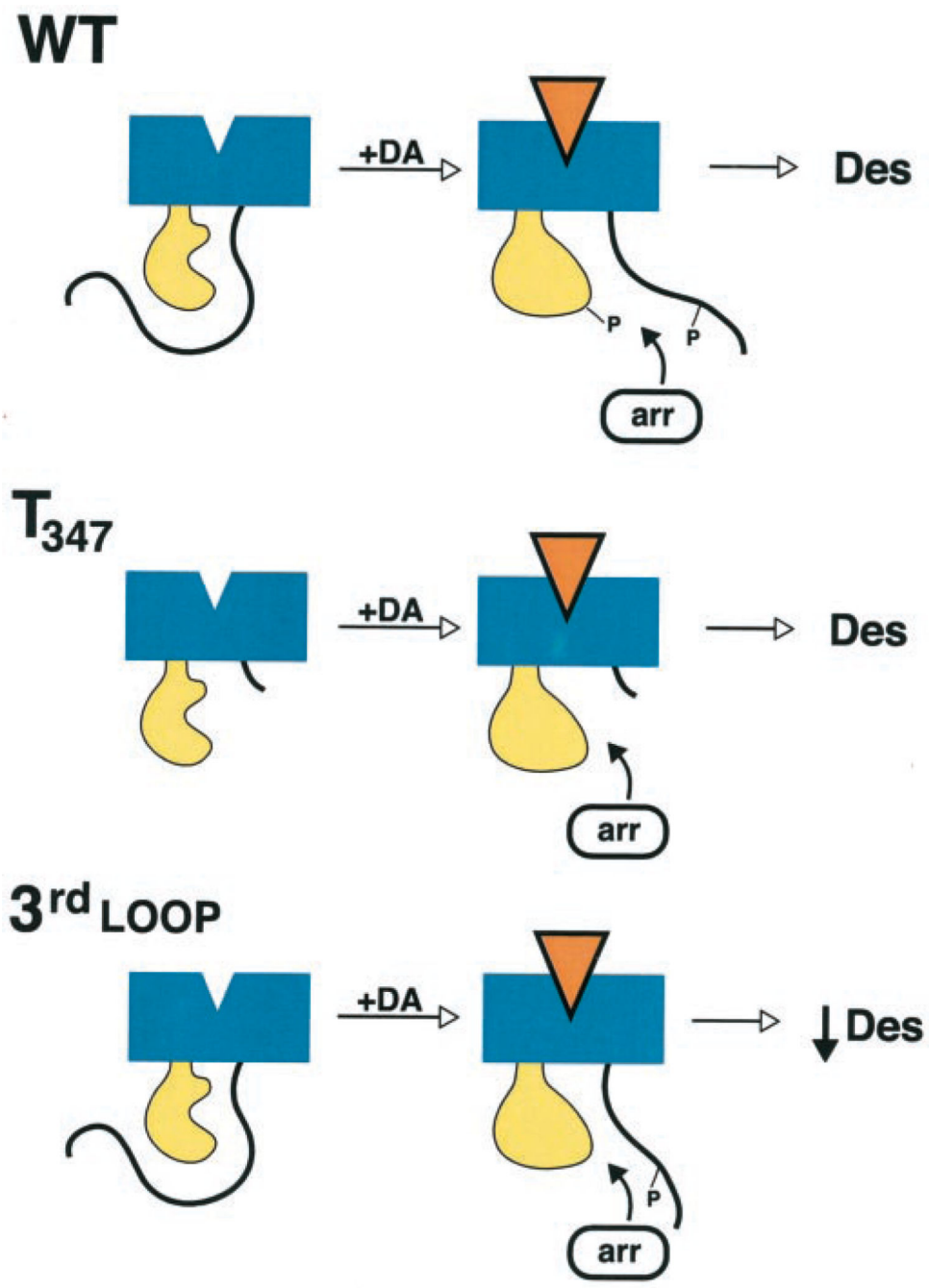

Fig. 14. Hypothetical scheme for receptor phosphorylation and arrestin binding to wild-type (*WT*) and mutant D_1 receptors

See text for explanation.